



Published in final edited form as:

Pediatr Blood Cancer. 2013 March ; 60(3): 377–382. doi:10.1002/pbc.24210.

The Application of Radiation Therapy to the Pediatric Preclinical Testing Program (PPTP): Results of a Pilot Study in Rhabdomyosarcoma

Rita Kaplon, BS^{#1}, Mersiha Hadziahmetovic, MD^{#1}, Jim Sommerfeld, BS¹, Kathryn Bondra, BS¹, Lanchun Lu, PhD¹, Justin Leasure, BS¹, Phuong Nguyen, MD¹, Kelsey McHugh, BS¹, Ning Li, MD, PhD¹, Christopher Chronowski, BS¹, Nikhil Sebastian, BS¹, Mamta Singh, PhD¹, Raushan Kurmasheva, PhD², Peter Houghton, PhD², and Christopher E. Pelloski, MD^{1,2,*}

¹Wexner Medical Center at The Ohio State University, Arthur G. James Comprehensive Cancer Center and Richard L. Solove Research Institute, Columbus, Ohio

²Nationwide Children's Hospital, Columbus, Ohio

These authors contributed equally to this work.

Abstract

Background—The Pediatric Preclinical Testing Program (PPTP) has been successfully used to determine the efficacy of novel agents against solid tumors by testing them within a mouse-flank in vivo model. To date, radiation therapy has not been applied to this system. We report on the feasibility and biologic outcomes of a pilot study using alveolar and embryonal rhabdomyosarcoma xeno-graft lines.

Procedures—We developed a high-throughput mouse-flank irradiation device that allows the safe delivery of radiotherapy in clinically relevant doses. For our pilot study, two rhabdomyosarcoma xenograft lines from the PPTP, Rh30 (alveolar) and Rh18 (embryonal) were selected. Using established methods, xenografts were implanted, grown to appropriate volumes, and were subjected to fractionated radiotherapy. Tumor response-rates, growth kinetics, and event-free survival time were measured.

Results—Once optimized, the rate of acute toxicity requiring early removal from study in 93 mice was only 3%. During the optimization phase, it was observed that the alveolar Rh30 xenograft line demonstrated a significantly greater radiation resistance than embryonal Rh18 in vivo. This finding was validated within the standardized 30 Gy treatment phase, resulting in overall treatment failure rates of 10% versus 60% for the embryonal versus alveolar subtype, respectively.

*Correspondence to: Christopher E. Pelloski, MD, Wexner Medical Center at The Ohio State University, Arthur G. James Comprehensive Cancer Center and Richard L. Solove Research Institute, 300 West 10th Avenue, Suite 094A, Columbus, OH 43210-1280. christopher.pelloski@osumc.edu.

Conflict of interest: Nothing to declare.

Conclusions—Our pilot study demonstrated the feasibility of our device which enables safe, clinically relevant focal radiation delivery to immunocompromised mice. It further recapitulated the expected clinical radiobiology.

Keywords

fractionated radiotherapy; PPTP; preclinical testing; rhabdomyosarcoma; xenograft

INTRODUCTION

The Pediatric Preclinical Testing Program (PPTP) is a well-established initiative that employs panels of pediatric solid tumor and leukemia xenograft models that recapitulate the clinical experience with commonly administered chemotherapeutic agents in a variety of childhood malignancies. It, therefore, currently serves as a valuable model to test the efficacy of novel agents, and has a strong record of correctly predicting the responses of various malignancy types to standard and novel therapies that are observed in the clinical setting [1–4]. Seventy-five percent of PPTP models have been derived from direct transplant of tumor tissue into mice, hence tissue culture artifacts have been avoided. Some reports have suggested that these procedures preserve tumor initiating cells when tumor fragments are directly implanted within the flanks of severe combined immunodeficient (SCID) mice [5,6]. The influence of tumor/tissue environment is preserved when using xenografts (which include stromal and tumor initiating cells of the original tumor). Xenograft models are thus favored over in vitro conditions for robust drug efficacy screening, due to these better recapitulated “real-world” phenomena [7–9]. For these reasons, the histologic as well as molecular phenotypes of the PPTP disease models remain preserved after multiple passages within these mice [10,11].

Prior to this report, no radiotherapy studies have been performed using this model. Incorporating radiotherapy into candidate drug screening provides an extra dimension to this process, as it allows for the identification of potential synergism and/or enhanced toxicity within a living system. More broadly, given the robust recapitulation of the clinical biology demonstrated by the panels of tumor xenografts, applying radiation will enable a comprehensive investigation of mechanisms of radiation resistance across a wide spectrum of pediatric malignancies. Similar to the improved drug efficacy prediction with in vivo models (vs. in vitro testing), radiotherapy has been shown to follow suit [12].

Historically, radiobiology research has been removed from the clinical experience. The cells of traditional radiobiology assays (notably, the clonogenic survival assay) are grown in tissue culture dishes. The in vitro passaging artifact results in cells that bear little molecular resemblance of the cells from whence they came [13,14]. Delivering clinically relevant radiation dosing and scheduling to large numbers of small animals or other in vivo pediatric cancer models has proven to be technically challenging as well. Investigators have attempted to circumvent these difficulties by either using very few numbers of experimental subjects, or delivering large, single-dosed fractions, oftentimes to the entire animal. This further removes applicability to the radiation treatment of children, given that most pediatric radiotherapy regimens require focal doses, between 1.5 and 2.0 Gy per fraction. While still

under investigation, early reports indicate that the molecular changes from conventional fractionation and large-single doses have almost divergent molecular radiobiology and response characteristics [15–17]. Recently, mouse-flank models have been used for in vivo fractionated radiotherapy experiments for various adult tumors [18–21], but this approach has yet to be employed in the study of pediatric cancers. To improve the efficacy of treatment regimens in pediatric cancer and elucidate the relevant radiobiology that governs treatment failures, inclusion of radio-therapy within the in vivo preclinical testing phase is paramount.

To address these current shortcomings, we have designed a custom irradiation device that allows high-throughput flank irradiation, for large numbers of SCID mice. In this report, we describe the feasibility of this approach as well as the radiobiologic metrics of our pilot study, using alveolar and embryonal rhabdomyosarcoma xenograft lines.

MATERIALS AND METHODS

Mouse-Flank Irradiation Apparatus

The apparatus consists of a semi-sealed acrylic box and individual shielding units for each mouse (Fig. 1A–C). The box is approximately 35 cm × 35 cm 7 × cm to fit the RadSource RS2000 laboratory irradiator. It has an air intake valve so that isoflurane and oxygen levels can be maintained within the compartment. The individual shielding units are acrylic tubes covered in 1.63 mm lead foil. Each tube has a cut-out and platform to allow an anesthetized mouse's body to be protected within the tube, while the left leg is extended immobilized, exposing the flank xenograft. Lead head caps and additional foil with pre-cut circular collimation to create a 2–3 mm surface margin of beam exposure were then added to cover all unshielded areas. The individual units were shaped so that all five xenografts were aligned within the base of the beam cone, equidistant from the beam center, to ensure an approximate equal dose-rate. With a single unit (after the anesthetic induction of mice), up to 60 mice per hour can be irradiated. [For more detailed fabrication plans, please personally contact the corresponding author.]

We used the RS 2000 X-ray Biological Irradiator (Rad Source Technologies, Inc., Suwanee, GA) to irradiate the mice. The machine was run at 160 kVp and 25 mA with its standard 0.3 mm of Cu filtration. The X-ray generated under this condition had an energy spectrum with the minimum energy of 45 kV up to maximum 160 kV, and the half value of the beam was 0.62 mm of Cu. The dose gradient of this X-ray in tissue-equivalent bolus was about –10% per 0.5 cm depth. Quality assurance of the shielding and xenograft dosing was performed using nanoDot dosimeters (Landauer, Inc., Glenwood, IL). Dose readings at xenograft surfaces and with layered bolus phantoms were used to calculate the appropriate “beam-on” treatment times. Dosimeters placed at the throat, back, and under the abdomen of animals undergoing treatment and were compared to the doses received by the xenograft (unshielded) to determine the percent blockage of non-targeted animal by the device. These dosimeters were calibrated under the beam conditions described above.

Daily Irradiation Procedure and Dose Measurements

Groups of five mice were anesthetized at once in an induction chamber with continuous 5% isoflurane and 4 L/min O₂. The treatment device received this same anesthetic gas mixture and flow-rate during mouse loading and treatment as well. Anesthetized mice were removed one at a time from the induction chamber and placed in their individual units with shielding added as described above. Five mice would then undergo a single 2 Gy fraction and subsequently were removed from anesthesia and allowed to recover in warm conditions. From induction to recovery the mean treatment time, once optimized, was 10 minutes.

Xenograft Lines and Mice

The xenograft lines used were two rhabdomyosarcoma (RMS) lines: Rh18 (embryonal) and Rh30 (alveolar), which were harvested at diagnosis and engrafted into mice prior to the donor patient having received any cytotoxic therapy. These lines were created directly from patient samples propagated in mice-only and were never grown in vitro. These two lines express distinct genotypes; Rh30 expresses the fusion transcription factor PAX3-FKHR (present in 70% of alveolar RMS) while Rh18 does not. This distinction was confirmed via RT-PCR for the fusion product (data not shown). After implantation, xenografts were allowed to grow until reaching approximately 0.5–1.0 cm³ in volume and were then randomized to treatment or control (no treatment) groups; with the first measurement representing Day 0 of experiments.

CB17SC *scid*^{-/-} female mice (Taconic Farms, Germantown, NY), were used to propagate subcutaneous tumors. All mice were maintained under barrier conditions and experiments were conducted using protocols and conditions approved by the institutional animal care and use committee of The Ohio State University (IACUC protocol 2010A00000192 [effective 3-year approval period: 12/28/2010–12/28/2013]). Female mice were used irrespective of the gender from which the tumor was derived. Tumor volumes (cm³) were determined weekly, to determine growth and response, as previously described [1].

Metrics, Endpoints, and Statistics

In addition to tumor growth kinetics, the complete response (CR) rates, recurrence rates, and 12-week failure rates were ascertained. A CR was defined as a complete xenograft disappearance during/ after treatment. A recurrence was defined as a measureable xeno-graft reappearing after at least 1 week of CR and followed by at least 2 weeks of growth. A 12-week treatment failure was either the lack of complete response or recurrence within the 12-week post-treatment observation period. Animal event-free survival was ascertained and defined from the time of treatment initiation (or beginning of observation for controls) until the time at which animals were removed from the study for the following events: (1) when xenografts reached four times their relative volume (final tumor volume/initial volume); (2) the absolute volume exceeded 2.5 cm³; and/or (3) the xenograft grew to severely impede mobility or comfort of the subject mouse. Treatment-related events were defined as animals which failed to complete the study due to excessive treatment toxicity which warranted early removal.

Statistical Methods

Differences in event-free survival times among groups were compared using the log-rank method. Actuarial complete response rates, recurrence rates and 12-week treatment failure rates between groups were compared using the Fisher's exact test. The differences between the means of groups were compared using a Student's *t*-test. Additionally, since a range of radiation doses and initial xenograft volumes were used, a unit of the given radiation dose divided by volume (cm³) of the initial xenograft size (dose-density, Gy/cm³) was used to compare for any dose-volume differences that may have affected outcomes. This is based on the radiobiologic principle that the likelihood of complete tumor eradication, for a given dose, is partially dependent on the number of cells present at the inception of treatment [22,23].

RESULTS

Apparatus Physics Quality Assurance

The custom irradiation apparatus made it possible to irradiate five mice at a time while minimizing prohibitive side effects from daily radiation and anesthesia exposure. To estimate the minimum doses to the base of the xenograft, a 0.5 cm bolus was used to approximate the implanted tumor size at the initiation of treatment. The measured dose at 0.5 cm depth of tissue equivalent bolus, with 1.0 cm circular collimation (most frequently used size) was 202 cGy (range 193–221 ± cGy) at an approximate dose-rate of 285 cGy/minute. With 2.5 cm circular collimation (for the largest initial tumors), the measured dose was 221 cGy (range 214–26 ± cGy). These slightly higher doses were deemed acceptable, given that in the clinic the maximum point dose is often higher than the target dose due to practice of prescribing to isodose lines to encompass volumes (with maximum point doses often between 7% and 12% higher than the prescribed dose). Measurements of doses received by the shielded, non-targeted animal, relative to the unshielded xenograft doses were 4.2% (±0.6%) under the abdomen, 2.0% (±0.3%) and 2.2% (±0.2%) for the back, representing 95.8–98.0% shielding for all anatomic sites (Fig. 1D).

Optimization Phase

Seventy-eight mice comprised the optimization phase. During this phase, various radiation doses were delivered to the flanks of xenograft-bearing mice for both assessment of the prototype device performance, implantation technique, general responsiveness of xenografts, treatment and animal tolerance of fractionated radiotherapy. The initial treatment-related toxicity rates were unacceptable. Twenty-six (33%) developed acute toxicity that required early removal from studies. The majority of these were due to excessive skin reaction or genitourinary (GU) dysfunction (Table I). GU dysfunction manifested as uterine/vaginal prolapse or excessive desquamation over the genital/urethral region; both of which resulted in distressed self-grooming which warranted early removal from study. We also noticed that smaller mice (<12 g) tended to fair worse than their larger counterparts (data not shown). This most likely resulted in a larger percent of the animal receiving target and non-target doses (higher body integral dose). To address these high toxicity rates, the non-targeted animal shielding was modified, increasing it to essentially a non airgap coverage with pre-cut circular lead foil collimation (0.50, 0.75, 1.00, 1.25, 1.50 2.0, and 2.5 cm diameter

aperture) centered over the xenograft. Tumors were implanted through an incision at the mid-upper left hind leg, which was more lateral than the customary dorsal/spinal approach (reducing the likelihood of medial engraftment, which could lead to increased target dose spill-over into the abdominal cavity), and only mice >16 g were used. These improvements essentially eliminated GU dysfunction. Further, skin care and weight maintenance were improved with the ad lib use of: sterile Bacon Flavored-Rimadyl tablets (2 mg/tablet) and Supreme Mini-Treats (Bioserve, Beltsville, MD); Buprenex (Reckitt Benckiser, Parsippany-Troy Hills, NJ); Meta-cam (Boehringer Ingelheim, Ridgefield, CT); and Diet Gel (Cincinnati Lab Supply, Cincinnati, OH) before, during and after treatments. Lastly, a more controlled anesthesia delivery system for all phases (induction, treatment, and recovery) was implemented as well.

After implementing these changes, 93 mice have since been treated (for this study and others, including co-administration with chemotherapies) and the rate of treatment-related study removal has dropped significantly, (acute toxicity-related early removal criteria improved from 33% to 3%; Table I). One group of five mice was able to tolerate up to 40 Gy in 20 fractions with no early toxicity events occurring before the 12-week observation period (data not shown).

In the optimization phase, there were a sufficient number of mice bearing the Rh30 and Rh18 xenografts to compare their inherent radiosensitivities. After eliminating the mice which succumbed to early treatment toxicities, 18 mice which harbored Rh30 and 12 mice which harbored Rh18 xenografts were identified as evaluable for the assessment of 12-week treatment failure rates. The 12-week treatment failure rates within the Rh30 group was 14/18 (78%) while 3/12 (25%) within the Rh18 failed ($P = 0.006$, Fisher's exact). There was no significant difference between the mean time to recurrence of the Rh30 (49 ± 9 days) and Rh18 (53 ± 6 days) groups. No significant difference was noted between the mean dose densities of the Rh30- and Rh18-bearing mice groups (60 Gy/cm^3 vs. 59 Gy/cm^3 , respectively) either.

Standardized Dosing Phase

The preliminary optimization-phase result suggested that the embryonal tumor (Rh18) was more radiation sensitive than the alveolar models (Rh30). To validate the preliminary observation, a dose of 30 Gy in 15 fractions was given to groups of mice bearing the Rh30 and Rh18 xenografts while separate, untreated groups represented the controls (10 mice per group). For both treatment groups, the addition of radiotherapy significantly improved the overall event-free survival rate (17 days vs. 106 days, respectively, $P < 0.001$, log-rank; Fig. 2A). There were no acute treatment-related deaths. Both groups demonstrated a 10/10 complete response rate. There was one recurrence within the Rh18 group and 6/10 recurrences in the Rh30 group, resulting in a 12-week treatment failure rate of 1/10 versus 6/10 (for Rh18 and Rh30 groups, respectively, $P = 0.029$, Fisher's exact; Fig. 3A–D). Inspection of Figure 2B reveals that there was a trend in improved event-free survival between the Rh18 versus the Rh30 group (log-rank, $P = 0.072$; the median could not be determined for the Rh18 group due to only 1 event occurring during the observation period). No significant difference was noted between the mean dose densities of the Rh30- and

Rh18-bearing mice groups in the standard treatment phase as well (80 Gy/cm³ vs. 87 Gy/cm³, respectively).

DISCUSSION

The continued suboptimal clinical outcomes in children who receive radiation therapy for their solid tumors, coupled with the profound lack of a thorough understanding of the molecular/biologic effects of radiation upon these tumors create an urgent need for improvement in this area. Children are the most at-risk patient population with regards to radiotherapy. Treatment failure and premature death from cancer comes at an enormous cost for the families who endure this challenge and for society as a whole, considering that the average-years of life lost in the US due to cancer in 2007 was highest (71 thousand years) for the pediatric (ages 0–14) population (<http://progressreport.cancer.gov>). The importance of improved radiation efficacy and safety in children is further underscored when considering that radiation therapy is heavily utilized in the treatment of the more lethal pediatric tumors (high-grade CNS, sarcomas, neuroblastoma, etc.), which account for the bulk of the cancer-related mortality rates within this age-group. The long-term impact of radiotherapy can have devastating consequences on the survivors, as well. These consequences include impairments in IQ, growth retardation, organ dysfunction and the development of secondary malignancies; all of which hold a direct correlation to the integral and maximal radiation doses received [24,25]. Because of its late toxicity potential, attempts to scale back radiation dose or the removal of this modality entirely, based on population or clinical characteristics, has been met with increased treatment failures, especially when gross/measurable disease is present [26]. Only by incorporating radiotherapy into robust in vivo models, like the PPTP, can there be discovery of relevant radio-resistance mechanisms and their predictive biomarkers, as well as the comprehensive preclinical testing within the context of novel agents. It is anticipated that this approach will ultimately lead to more rational, safe and efficacious uses of this modality in children stricken with cancer.

For our pilot study, we selected two xenograft lines representing the two most common subtypes of pediatric RMS: alveolar (ARMS; Rh30) and embryonal (ERMS; Rh18). The former is the most biologically aggressive subtype of this disease, confers a 5-year overall survival of <50% (10–30% when metastatic at presentation), and requires higher doses of radiation to be delivered across all stages and surgical groupings when compared to the more favorable ERMS, which confers a 73% 5-year overall survival [27]. Despite progress made in this disease, control of the primary site is still a major source of treatment failure, as 2/3 of the relapses observed in Intergroup RMS Study-IV (n = 888) were local-regional [28], suggesting an inherent resistance to radiotherapy in this disease. The biologic results of this pilot study recapitulate this clinical experience. The ARMS line, harboring the characteristic PAX3:FKHR translocation was clearly the more resistant than the ERMS line. Thus, as previously demonstrated with successful preclinical testing of novel and standard systemic agents within the PPTP panel, radiation therapy appears to have a similar biologic reproducibility in this model.

In general, as more genetic alterations driving the malignant process are discovered, it is extremely important to have animal models that recapitulate these alterations in order to

develop effective targeted agents. Animal models using murine or human tumor grafts in to isogenic hosts or immune-deficient animals have been used for years to predict efficacy and toxicities of chemotherapeutic and, lately, targeted agents. However, no successful small animal model exists to predict efficacy of radiation as delivered in the conventional clinic setting for pediatric cancers. Our pilot study shows that radiotherapy can be effectively applied to the PPTP system and reliably recapitulates the clinical experience with external beam radiotherapy using reproducible, daily conventional fractionation. We anticipate extending this approach across the other malignancies of the PPTP in the near future.

ACKNOWLEDGMENT

The work was supported through a Hope On Wheels Programmatic grant from the Hyundai Corporation of North America, and an NIH award NO1-CM-42216 from the National Cancer Institute. The authors thank Irene Snyder for her assistance in manuscript and figure preparation.

Grant sponsor: Hyundai Corporation of North America; Grant sponsor: National Cancer Institute; Grant number: NO1-CM-42216.

REFERENCES

1. Houghton PJ, Morton CL, Tucker C, et al. The pediatric preclinical testing program: Description of models and early testing results. *Pediatr Blood Cancer*. 2007; 49:928–940. [PubMed: 17066459]
2. Houghton PJ, Morton CL, Kolb EA, et al. Initial testing (stage 1) of the mTOR inhibitor rapamycin by the pediatric preclinical testing program. *Pediatr Blood Cancer*. 2008; 50:799–805. [PubMed: 17635004]
3. Houghton PJ, Morton CL, Kolb EA, et al. Initial testing (stage 1) of the proteasome inhibitor bortezomib by the pediatric preclinical testing program. *Pediatr Blood Cancer*. 2008; 50:37–45. [PubMed: 17420992]
4. Kolb EA, Gorlick R, Houghton PJ, et al. Initial testing (stage 1) of a monoclonal antibody (SCH 717454) against the IGF-1 receptor by the pediatric preclinical testing program. *Pediatr Blood Cancer*. 2008; 50:1190–1197. [PubMed: 18260118]
5. Yu L, Baxter PA, Voicu H, et al. A clinically relevant orthotopic xenograft model of ependymoma that maintains the genomic signature of the primary tumor and preserves cancer stem cells in vivo. *Neuro Oncol*. 2010; 12:580–594. [PubMed: 20511191]
6. Shu Q, Wong KK, Su JM, et al. Direct orthotopic transplantation of fresh surgical specimen preserves CD133+ tumor cells in clinically relevant mouse models of medulloblastoma and glioma. *Stem Cells*. 2008; 26:1414–1424. [PubMed: 18403755]
7. Hoffman RM. In vitro sensitivity assays in cancer: A review, analysis, and prognosis. *J Clin Lab Anal*. 1991; 5:133–143. [PubMed: 2023059]
8. Carney DN, Winkler CF. In vitro assays of chemotherapeutic sensitivity. *Importance Adv Oncol*. 1985:78–103. [PubMed: 3916747]
9. Yung WK. In vitro chemosensitivity testing and its clinical application in human gliomas. *Neurosurg Rev*. 1989; 12:197–203. [PubMed: 2682352]
10. Neale G, Su X, Morton CL, et al. Molecular characterization of the pediatric preclinical testing panel. *Clin Cancer Res*. 2008; 14:4572–4583. [PubMed: 18628472]
11. Whiteford CC, Bilke S, Greer BT, et al. Credentialing preclinical pediatric xenograft models using gene expression and tissue microarray analysis. *Cancer Res*. 2007; 67:32–40. [PubMed: 17210681]
12. Deschavanne PJ, Fertil B. A review of human cell radiosensitivity in vitro. *Int J Radiat Oncol Biol Phys*. 1996; 34:251–266. [PubMed: 12118559]
13. Ross DT, Perou CM. A comparison of gene expression signatures from breast tumors and breast tissue derived cell lines. *Dis Markers*. 2001; 17:99–109. [PubMed: 11673656]

14. Lee J, Kotliarova S, Kotliarov Y, et al. Tumor stem cells derived from glioblastomas cultured in bFGF and EGF more closely mirror the phenotype and genotype of primary tumors than do serum-cultured cell lines. *Cancer Cell*. 2006; 9:391–403. [PubMed: 16697959]
15. Tsai MH, Cook JA, Chandramouli GV, et al. Gene expression profiling of breast, prostate, and glioma cells following single versus fractionated doses of radiation. *Cancer Res*. 2007; 67:3845–3852. [PubMed: 17440099]
16. Hamilton J, Higgins G, Bernhard EJ. Conventional radiotherapy or hypofractionation? A study of molecular changes resulting from different radiation fractionation schemes. *Cancer Biol Ther*. 2009; 8:774–776. [PubMed: 19395860]
17. Zelefsky MJ, Greco C, Motzer R, et al. Tumor control outcomes after hypofractionated and single-dose stereotactic image-guided intensity-modulated radiotherapy for extracranial metastases from renal cell carcinoma. *Int J Radiat Oncol Biol Phys*. 2011; 82:1744–1748. [PubMed: 21596489]
18. Blanquicett C, Saif MW, Buchsbaum DJ, et al. Antitumor efficacy of capecitabine and celecoxib in irradiated and lead-shielded, contralateral human BxPC-3 pancreatic cancer xenografts: Clinical implications of abscopal effects. *Clin Cancer Res*. 2005; 11:8773–8781. [PubMed: 16361565]
19. Jarnagin WR, Zager JS, Hezel M, et al. Treatment of cholangiocarcinoma with oncolytic herpes simplex virus combined with external beam radiation therapy. *Cancer Gene Ther*. 2006; 13:326–334. [PubMed: 16138120]
20. Moyer JS, Li J, Wei S, et al. Intratumoral dendritic cells and chemoradiation for the treatment of murine squamous cell carcinoma. *J Immunother*. 2008; 31:885–895. [PubMed: 18832999]
21. Sarkaria JN, Carlson BL, Schroeder MA, et al. Use of an orthotopic xenograft model for assessing the effect of epidermal growth factor receptor amplification on glioblastoma radiation response. *Clin Cancer Res*. 2006; 12:2264–2271. [PubMed: 16609043]
22. Thames HD, Suit HD. Tumor radioresponsiveness versus fractionation sensitivity. *Int J Radiat Oncol Biol Phys*. 1986; 12:687–691. [PubMed: 3700173]
23. Brenner DJ. Dose, volume, and tumor-control predictions in radiotherapy. *Int J Radiat Oncol Biol Phys*. 1993; 26:171–179. [PubMed: 8482624]
24. Ishida Y, Sakamoto N, Kamibeppu K, et al. Late effects and quality of life of childhood cancer survivors: Part 2. Impact of radiotherapy. *Int J Hematol*. 2010; 92:95–104. [PubMed: 20577841]
25. Armstrong GT, Stovall M, Robison LL. Long-term effects of radiation exposure among adult survivors of childhood cancer: Results from the childhood cancer survivor study. *Radiat Res*. 2010; 174:840–850. [PubMed: 21128808]
26. Skowronska-Gardas A. A literature review of the recent radiotherapy clinical trials in pediatric brain tumors. *Rev Recent Clin Trials*. 2009; 4:42–55. [PubMed: 19149762]
27. Ognjanovic S, Linabery AM, Charbonneau B, et al. Trends in childhood rhabdomyosarcoma incidence and survival in the United States, 1975–2005. *Cancer*. 2009; 115:4218–4226. [PubMed: 19536876]
28. Crist WM, Anderson JR, Meza JL, et al. Intergroup rhabdomyosarcoma study-IV: Results for patients with nonmetastatic disease. *J Clin Oncol*. 2001; 19:3091–3102. [PubMed: 11408506]

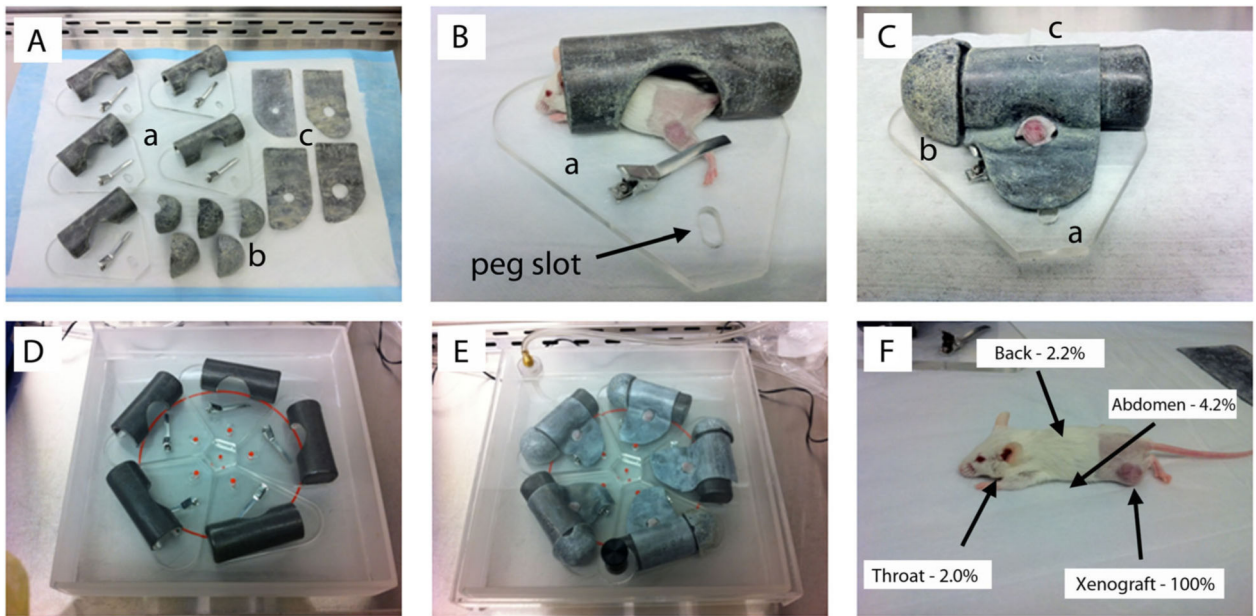


Fig. 1.

Schematic of the mouse irradiation device and shielding efficiency. **A:** Individual mouse treatment chambers and component parts: (a) primary lead-shielded chamber with low-pressure left leg clamp; (b) lead head caps; and (c) lead flank shields with pre-cut circular collimation. **B:** Initial anesthetized mouse positioning within the body chamber with leg clamp engaged. **C:** Fully shielded individual chamber, with circular cut-out collimation for left flank/leg xenograft exposure. **D:** Five-chamber arrangement (with mice and components not included). The red circle identifies the edge of the beam cone. The small red dots are the tops of the pegs for position reproducibility. Xenografts were aligned equidistant from the beam center and within the cone to ensure a uniform dose-rate (approximately 285 cGy/minute) and total dose delivery per fraction. **E:** Complete set-up prior to treatment. The semi-sealed treatment box with inhalational anesthesia gas tubing attached to lid valve. **F:** Shielding quality assurance results based on body location. Measurements of doses received by the shielded, non-targeted animal, relative to the unshielded xenograft doses revealed 95.8–98.0% shielding for all anatomic sites.

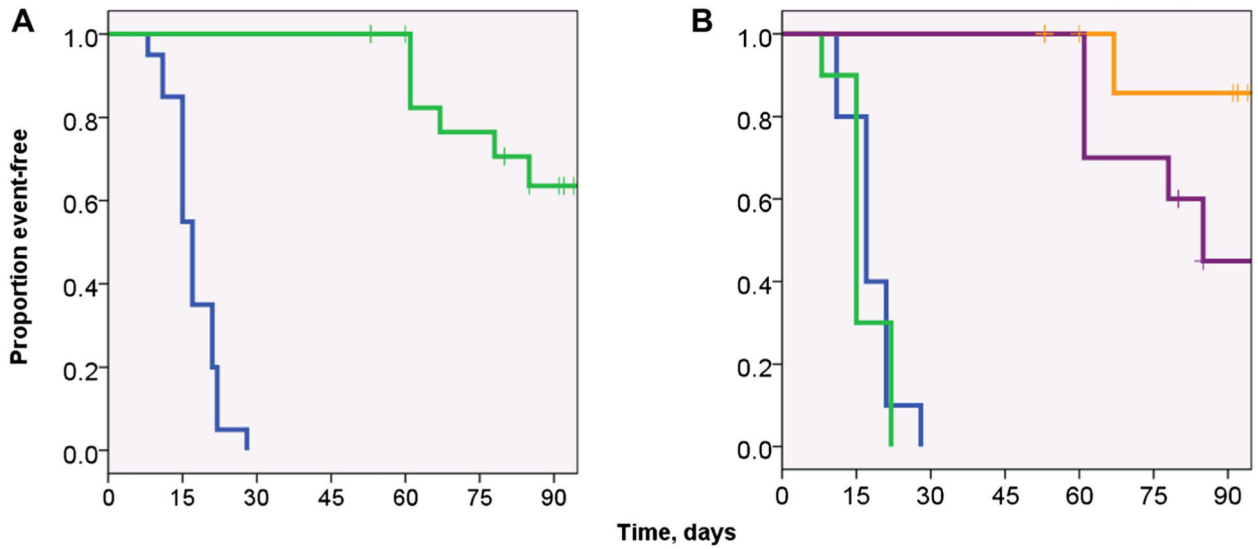


Fig. 2.

Kaplan–Meier event-free survival (EFS) curves of the standard radiotherapy dosing treatment groups. **A:** EFS curves of non-irradiated mice (blue line) versus irradiated (green line) with implanted xenografts (median EFS was 15 days versus 75 days for untreated versus treated mice, respectively [$P < 0.001$]). **B:** Event-free survival irradiated versus non-irradiated mice, stratified by xenograft line. There was no significant difference between the untreated groups (Rh18 and Rh30 controls, blue and green lines, respectively). There was a trend in improved EFS in the treated Rh18 group (orange line) versus the treated Rh30 group (purple line, $P = 0.072$; log-rank). The median survival of Rh18 group could not be calculated due to the lack of events within the 12-week observational period. *Note:* After implantation, xenografts were allowed to grow until reaching approximately $0.5\text{--}1.0\text{ cm}^3$ in volume and were then randomized to treatment or control (no treatment) groups; with the first measurement representing Day 0 of experiments.

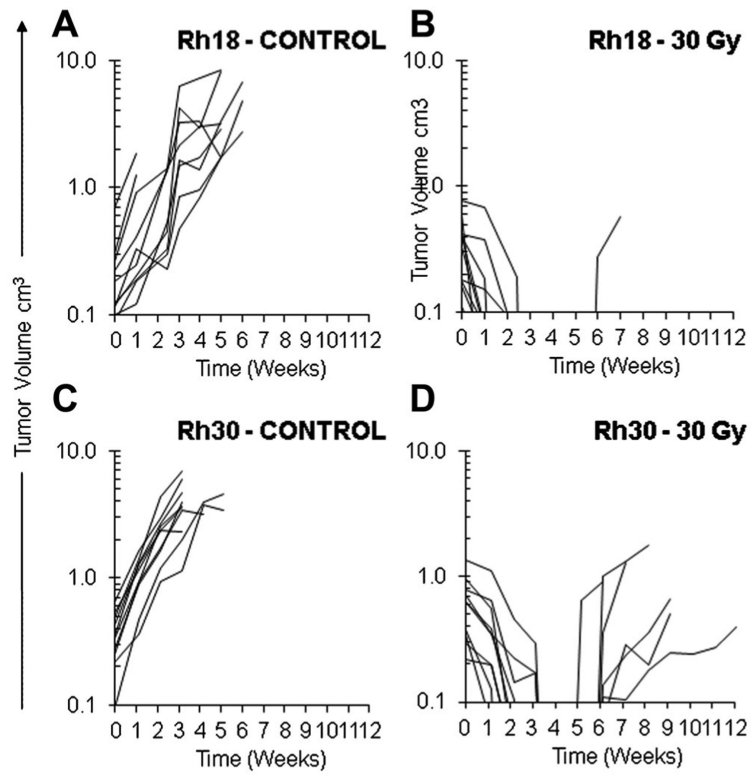


Fig. 3. Xenograft growth curves as a function over time in two rhabdomyosarcoma (RMS) lines in mice undergoing a standard radiotherapy dosing schedule (30 Gy in 15 fractions over 3 weeks) versus untreated controls. **A:** Rh18 (embryonal RMS) untreated; **B:** Irradiated Rh18 demonstrating one 12-week recurrence; **C:** Rh30 (alveolar RMS) untreated; **D:** Irradiated Rh30 demonstrating seven 12-week recurrences.

TABLE I

Animal Treatment Toxicity Rates During and After Device Optimization

	Anesthesia related	Desquamation, leg edema	GU dysfunction	Failure to thrive	Total deaths	Total treated	Treatment-related death rate (%)
Direct treatment effects—before optimization	2	12	8	4	26	78	33
Optimized	1	0	0	2 ^a	3	93	3

^aReceived chemo + radiation in a later study.

Author Manuscript

Author Manuscript

Author Manuscript

Author Manuscript